Estuarine Management and Technologies Journal

Estuarine Management and Technologies 2: 101–118 (2025)
DOI: 10.3897/emt.2.175774

Research Article

Influence of basement rock lithology on soil hydraulic conductivity and grain size distribution in lateritic soils of western Uganda: Implications for estuarine management

Haftay Hailu[1]

1 *Department of Land Resource Management and Environmental Protection, Water Resources and Irrigation Management, Mekelle University, P.O. Box: 231, Mekelle, Ethiopia*

Corresponding author: Haftay Hailu (haftay.hailu@mu.edu.et, haftishhailu@yahoo.com)

Abstract

The main focus of this study is to assess the control of grain size distribution, lithology, and depth on hydraulic conductivity (*K_Hazen*) within five weathered basement rocks (gneiss, gneiss-volcanics, quartzite, and granite) by means of statistical, regression, and mixed-effects modeling methods underpinned by hydrogeological interpretation. For this purpose, a total of 24 soil samples were analyzed using the GGU-SIEVE program, focusing on the determination of uniformity coefficient (Cu), coefficient of curvature (Cc), and hydraulic conductivity (*K_Hazen*). The investigation also included analysis of median-grain distribution, gradation, permeability, and soil type classifications, which are vital for sustainable soil management in regions with variable geological bedrocks, like in western Uganda. The results for Cu values range from 15 to 439, Cc ranges from 0.2 to 1.8, and K ranges from 5.8×10^{-8} to 1.3×10^{-4} m/s. These results demonstrate that the soils exhibit a wide range of textural variations and depth-dependent permeability trends. Gneiss-derived soils are permeable and exhibit moderate gradation. The quartzite and granite soils are more broadly graded but less porous, resulting from denser packing and finer matrix content. On the other hand, the gneiss-volcanics profile presents an intermediate characteristic due to mixed lithological influence. Based on statistical analysis, K decreases systematically with depth and is positively correlated with Cu and negatively with the percentage of fines. This is also confirmed by the model diagnostics, which suggest that K is jointly controlled by such factors as lithology, grain-size heterogeneity, and depth-dependent structure, with Cu emerging as a strong predictor, with the mixed-effects framework proving effective to model subsurface variability. These results underline the role of the controlling variables related to the parent rock and the intensity of weathering in influencing soil texture, gradation, shape (structure), and hydrologic response, which should be considered for erosion risk management, geotechnical study, and subsurface flow modeling in basement terrains.

Key words: Texture, Depth, Grading coefficients, Hydraulic behavior, Parent rock

OPEN ACCESS

Academic editor: Tri Soeprobowati
Received: 22 October 2025
Accepted: 22 November 2025
Published: 8 December 2025

Citation: Hailu H (2025) Influence of basement rock lithology on soil hydraulic conductivity and grain size distribution in lateritic soils of western Uganda: Implications for estuarine management. Estuarine Management and Technologies 2: 101–118. https://doi.org/10.3897/emt.2.175774

Copyright: © Haftay Hailu.
This is an open access article distributed under terms of the Creative Commons Attribution License (Attribution 4.0 International – CC BY 4.0).

Introduction

Estuarine environs are extremely dynamic, sensitive ecosystems, really influenced by land inputs and outputs such as direct surface runoff, sediment, and groundwater discharge and recharge. Within these hydrological catchments,

soil hydraulic properties play a vital role in governing contaminant transport, water transport, and nutrient leaching (Li et al. 2019; Fukushima et al. 2021). Lateritic soils are dominant in WU, which form under intense tropical weathering regimes further modified by the underlying bedrock. These soils meaningfully influence runoff formation, soil erosion processes, and sediment transportation rate, especially under high-intensity rainfall events. Soil physical properties, especially grain size distribution, grading parameters such as uniformity coefficient (Cu) and coefficient of curvature (Cc), as well as the hydraulic conductivity (*K_Hazen*), are largely determined by the parent material, as Fajobi et al. (2014) and Etim et al. (2025) reported. Basement rocks of WU, for example, granite, gneiss, quartzite, and gneiss-volcanic rocks, have distinctive mineralogical and textural contents producing heterogeneous soils with varying hydraulic behavior (Omara et al. 2018). For example, fine-textured parent materials, such as granite and gneiss, create soils with more clay and silt, resulting in reduced permeability and increased surface runoff, which increases erosion susceptibility (Obiefuna and Nur 2022; Amadi et al. 2023).

Conversely, coarse-textured soils, as more permeable, may cause sediment to be quickly transported into estuarine environments when vegetation is removed or land is disturbed (Tang et al. 2022). The degree of particle sorting, as indicated by Cu and Cc values, also affects soil structure and infiltration rate; the poorly graded soils (low Cu) tend to support low water infiltration and are highly susceptible to surface runoff (Lee et al. 2024; Etim et al. 2025; Waleed et al. 2025). This is particularly relevant in areas where land use changes, such as deforestation and agricultural expansion, restrict vegetative cover and increase erosion intensity (Amadi et al. 2023; Biru et al. 2025).

Despite the recognized importance of grain size parameters (Cu and Cc) and hydraulic characteristics to estuary and watershed management, a large knowledge gap still exists as far as understanding the effects of basement lithology on these characteristics in the study area. This gap needs to be filled in order to design effective soil conservation and water management techniques for river basins throughout the region. Therefore, the main focus of this study is to determine the controls of grain size parameter distribution, lithology, and depth on hydraulic conductivity within five weathered basement parent materials, using statistical, regression, and mixed-effects modeling approaches supported by hydrogeological interpretation. This includes the following specific objectives: 1) Quantification of the relationships among grain-size parameters (Cu and Cc), depth, and hydraulic conductivity (*K_Hazen*), by using correlation analysis along with exploratory plotting. 2) Using of grain-size metrics and depth to assess the predictive capability by fitting linear regression models and comparing their performance; 3) Testing the influence of lithology and profile-level variability by means of mixed-effects modeling, including random effects that take into account hierarchical geological structures as well as to compare different models with Akaike information criterion (AIC), Bayesian information criterion (BIC), log-likelihood ((LLF), and diagnostic plots to find the best modeling framework that fits this set of data; and 4) Explaining the observed patterns in grain-size variability and K across the five basement lithologies through integrated geological and hydrogeothecnical interpretation.

Materials and methods

Study area description and sample locations

The study site is in WU, which is geographically located astride the equator between 1°209'S and 2°209'N and 29°309'E and 32°059'E. The region forms part of the western boundary of the broad plateau of central Africa, which was uplifted between the eastern and western arms of the rift valley system during the mid-Tertiary (Nyende et al. 2014). The Rwenzori Range and lakes of the Western rift valley form a topographic periphery to the west and north, while the Victoria Nile, a major tributary of the White Nile, delimits the eastern boundary. The southern border is marked by the shoreline of Lake Victoria and by the international border with Tanzania and Rwanda. The Basement Complex, in western Uganda, comprises of an extensive groups of schists, marbles, gneisses and granulites with granitic and basic intrusions (Schlüter 2006). In addition to the predominant acid to intermediate gneisses and granulites, hornblende and pyroxene varieties are common. Though ultra-basic rocks are rare (Schlüter 2006), the dolerites and amphiboles are wide spread (Fig. 1).

Lateralization processes have led to the development of weathering mantles tens of meters thick, often capped with ferricretes (Taylar and Howard 1999) as a result of intense weathering of ferruginous shale. According to him, weathering can dissolved and washed away all the soluble minerals leaving behind hydrated Iron (III) oxide (laterites); and the remnants of laterites, certainly of Miocene age and possibly even older, cap many hill, and it is presumed that it has been formed on many surfaces until the present day.

Five weathering soil profiles exposed to major roads through construction activities and/or gully erosion were selected during a field campaign in western Uganda. Each profile was freshly cleaned before sampling, and samples were taken in such a manner as to cover all stratigraphic sequences.

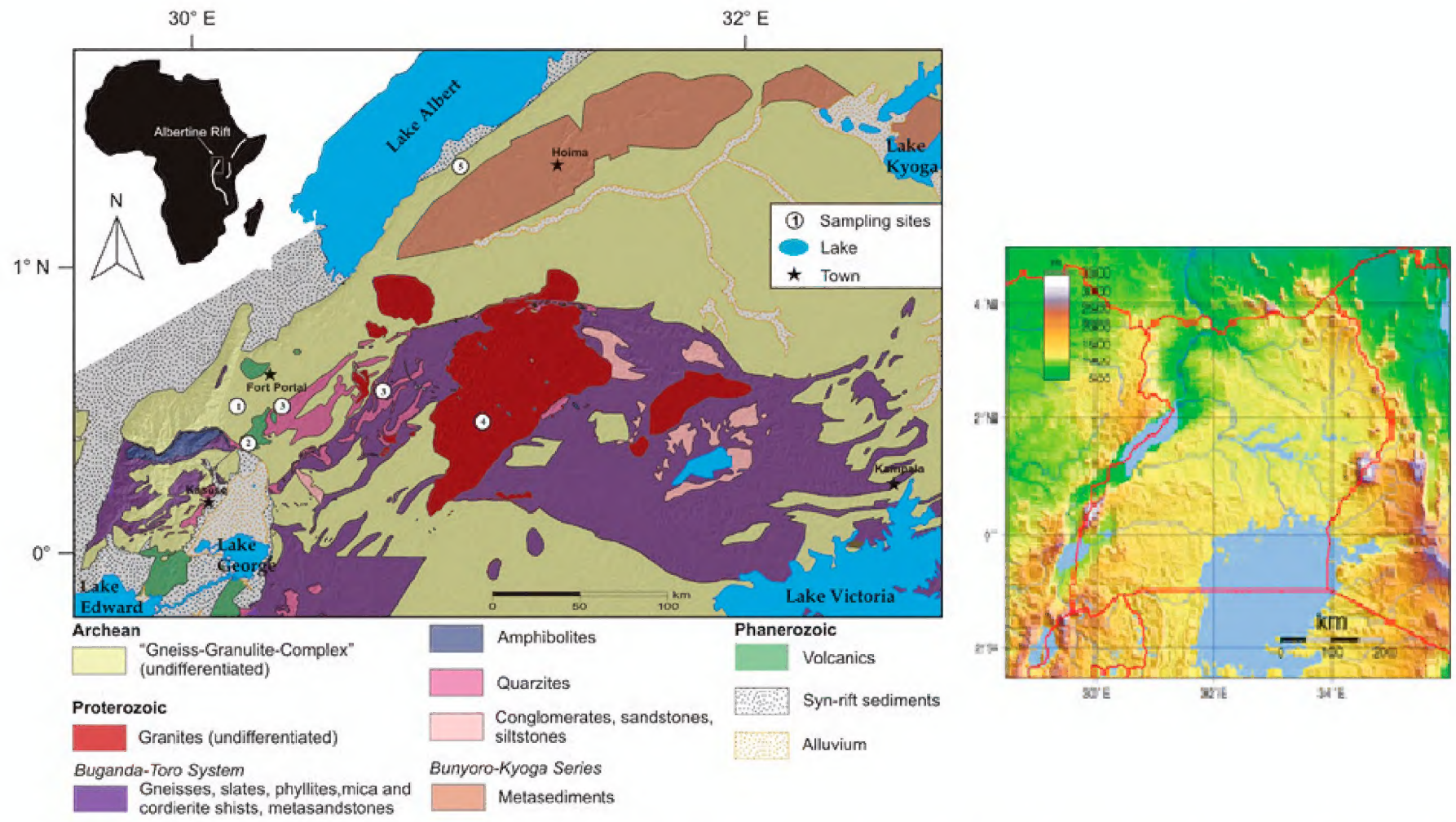

Figure 1. Location of soil samples on the geological map and topographic map (right) of western Uganda (Modified after Schlüter 2006).

Description of sampled soil profiles

The soils from gneisses (both S1 and S5) are more complex in texture, fine- to coarse-grained, composed of quartz, feldspars, amphiboles (mainly hornblende), and biotite. Their colour ranges from grey to light brown and in some places pink depending on the type of feldspar present (Fig. 2). This textural and colour due to drainage variation of the basement rock gneiss may cause the textural and colour variations in the soil.

Figure 2. Showing the distinct soil profiles developed on gneiss (S1 and S5), gneiss-volcanics (S2), quartzite (S3), and on granite (S4) in soils of western Uganda.

The soils sampled from profiles S1 and S5 are from the same basement of gneiss rock. However, profiles S1 and S5 were taken from nearly flat and near the top of the hill, respectively. Soil Profile S5 (near the hilltop) was dominated by red to orange colour, whereas soil profile S1 was dominated by gray/brown with yellowish subsurface. This colour difference depends on how well drained (how wet or dry) the profile is. The redder the soil, generally the better drained it is, as the water content controls the types of iron oxides that are present (Brown et al. 2004). This is why soils at or near the top the top of hill are quite red or orange, and progressively get more yellow and then brown towards the downhill (from soil profile S5 to S1 in the same basement gneiss rock). As Brown et al. (2004) explained, this transition is known as a 'toposequence'. There was a typical lateral (from higher in the landscape to lower in the landscape) difference between profiles S5 and S1 of gneiss basement rock in colour, permeability, texture, and porosity. This was due to the soil–landscape

patterns: (1) regular topography–geology relationships; (2) poor soil drainage on lower (S1) landscape positions; and (3) soil–landscape processes including erosion–deposition and hill-slope solute transport (Brown et al. 2004).

Some profiles show irregular, sometimes steeply dipping linear formations of gravel in profile S5 (Fig. 2), whose origin, according to different researchers such as Muller et al. (1981) and Colin et al. (1992), is not yet clear. The soil S1-1: 0.9 m depth is greyish-brown in colour, sandy with fine gravels, weak and friable, highly bioturbated with many medium and fine roots. This top profile S1 (S1-1) is stripped of much of its clay into S1-2 and S1-3 layers, and is thus lighter in colour than S1-2 and S1-3, which are beneath it (Fig. 2, S1). S1-1 is (eluviation) lower in clay content because of leaching. S1-3 is a zone of illuviation (accumulated substances-clay, iron, and aluminium compounds) that have been leached from overlaying layers. At S1-4 (4.5 m), the clay composition was reduced. This was due to the effect of the impermeable clay layer of illuviation overlaying it.

The gneiss-volcanic profile (S2) is about 5 m thick with four recognisable sequences (Fig. 2). About 3 m from the bottom, the sequence is highly crumbled with highly altered minerals, but still visible, and it is red in colour above, with fineness and clay content increasing towards the topmost layer with progressive changing of colour from red to darker shades of grey. The residual horizon, about 20 cm thick, is highly bioturbated. The sequences of soil horizons in this profile did not depend on the origin of the basement rock because of the volcanic activities and their depositions. The top horizon (S2-1) is characterized by very dark greyish-brown, gravely clayey sand, highly bioturbated, with medium and fine roots, very low porosity, and low hydraulic conductivity.

The soil profile S3 is mainly dominated by red colour (Fig. 2), which indicates the presence of hematite (Fe_2O_3). This profile is mainly dominated by sand and acidic soil. The soil profile (S4) also has a basement rock with interesting and beautiful light-colored rocks of granite. Quartz feldspars are the main components of this stone, with minor amounts of mica and amphibole minerals. The stage of weathering or alteration of the granites depends strongly on the structure and location of the rock. The massive, un-banded granites tend to be very fresh, and generally, the rock is less altered with distance from the escarpment. In other word, it is acidic rock that has a profound effect on the soil to make it acidic. The soil profile from the granite basement is about 8 m thick and typically red in colour. The profile S4 is cross-cut by quartz mineral veins (Fig. 2) at several points. The bottom sequence is strongly mottled and the minerals are greatly altered but still visible. The particle-size distribution (PSD), gradation (using Cu, Cc), and hydraulic conductivity are important soil parameters for detailed characterization and inter-profile comparisons of these profiles (S1 to S5).

Study site selection and sampling techniques

Five weathering soil profiles exposed to major roads through construction activities and/or gully erosion were selected during a field campaign in Uganda. Each profile lithologic (gneiss, granite, quartzite, volcanics) was freshly cleaned before sampling, and samples were taken in such a manner as to cover all stratigraphic sequences of the common basement rocks. The main purpose of choosing sampling sites was to obtain weathering profiles that

develop on these different basement rocks, including Archean gneisses of the Ugandan basement complex, granites and quartzite of the Proterozoic Buganda-Toro mobile belt, and Miocene highly mafic volcanics (Schlüter 2006), to characterize the soil property. Twenty-four soil samples were collected from each distinct lithologic site (labeled S1 to S5), i.e., in each profile, 3 to 6 samples were taken depending on the soil layering (horizonation) and colour, texture (particle size), structure, and other characteristics. These samples were obtained and labeled as S1-1, S1-2, to S5-5 at different depths (Table 1). Profiles were located and spaced at representative sites of each basement rack to ensure spatial independence. During the analysis of a soil profile, more attention is mainly focused on the subsoil horizons compared to the surface horizons, since surface horizons are often modified by human activities and thus may not reflect natural soil-forming processes. Therefore, the soils are composed of a succession of horizons, morphologically distinct layers that differ in appearance, thickness, structure, and properties. These differences are due to a variety of soil-forming processes. These horizons are roughly parallel to the land surface and form the soil profile. A soil profile, therefore, is a vertical section of the soil, a three-dimensional view that displays its layered nature.

Grain size distribution determination through sieve and sedimentation

One of the most important methods to characterize soil samples is the sieve analysis. The soil specimen was washed to separate fine grains from coarse grains. The samples were oven dried at 105 °C, weighed onto a 0.1% precision scale, after being sieved using a series of sieves by an agitating machine. The residue masses from each sieve after drying at 105 °C to their constant mass were determined. The shape of the grain size distribution was determined as per the standards of DIN 4022, which was supplemented by DIN ISO 11277, as highlighted in Buß (2025). It was conducted by separating the soil samples into their particle size fractions, using dry sieve analysis (for sizes > 0.063 mm) as well as sedimentation (for soil particle sizes < 0.03 mm) techniques (Fig. 3).

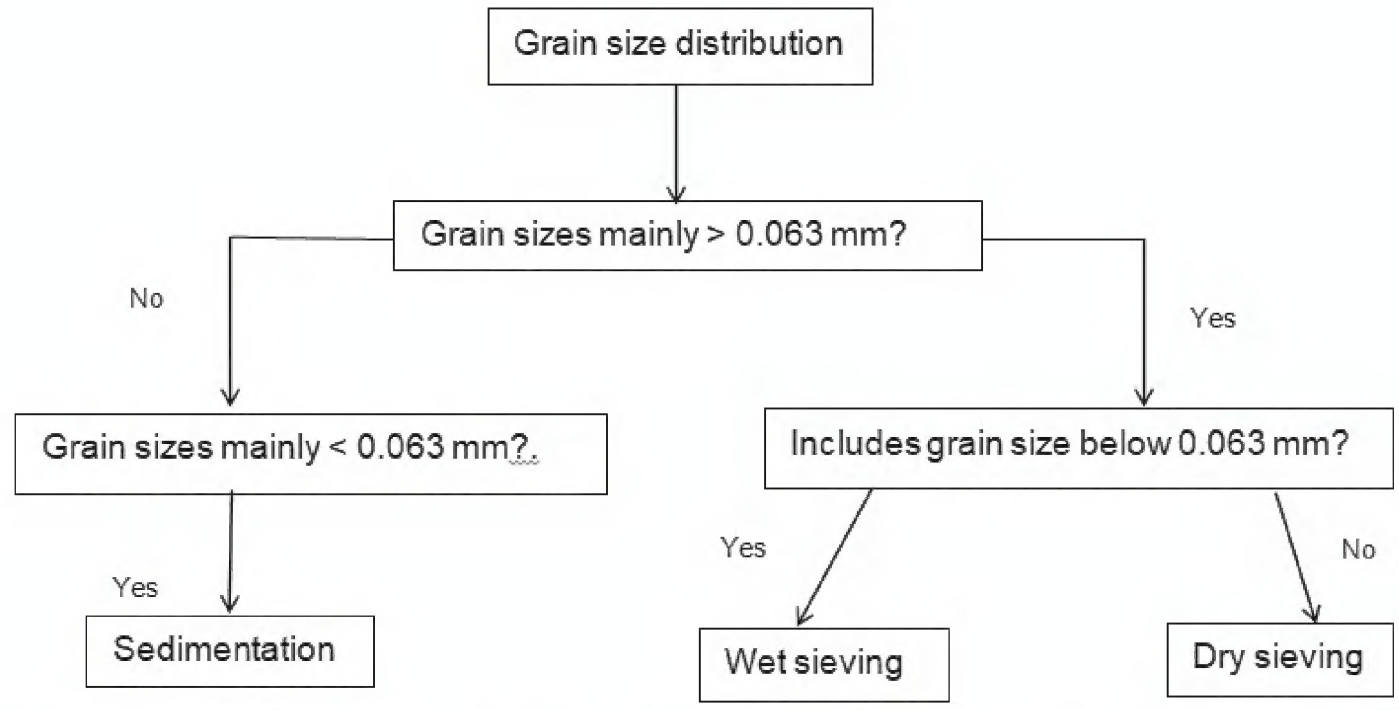

Figure 3. Illustrating the outlined methods for determining grain size distribution of soil samples

Combined sieving (dry and wet sieving) and sedimentation analysis were used to drive a continuous grain size distribution curve that is useful for soil classification and construction applications. Dry sieve analysis was conducted by passing the dried soil sample through a series of progressively finer sieves (usually ranging from 63 to 0.063 mm). The count weight of retained soil for every soil sample was computed to attain the proportion of coarse-grained grading (Fig. 4b).

a)

b)

Sieve #	Sieve Diam. (mm)		Weight of the Fraction (mg)	Content of the Fraction (%)	Percent Coarser than the Sieve Diameter
6	3.35		45.2	9.04	9.04
10	2.00		95.1	19.02	28.06
12	1.70		204.0	40.80	68.86
16	1.18		97.8	19.56	88.42
20	0.850		39.5	7.90	96.32
30	0.600		13.6	2.72	99.04
40	0.425		2.2	0.44	99.48
60	0.250		1.9	0.38	99.86
100	0.150		1.0	0.19	100.05
Bottom Pan	-		0.1	0.38	100.33

c)

d)

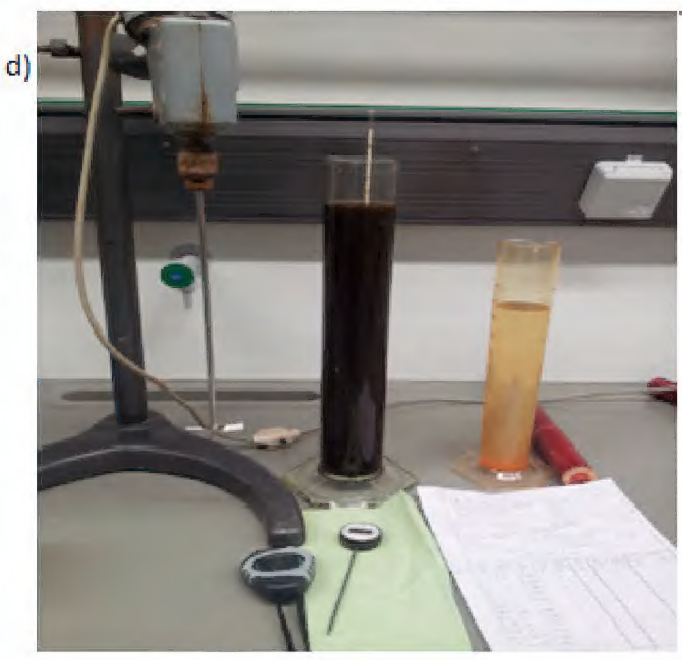

Figure 4. Illustrating the dry sieving (**a**), wet sieving (**c**), percent coarser than the sieve diameter (**b**), and hydrometer (**d**) methods for the determination of grain size distribution for a soil sample in western Uganda.

During the sedimentation test (hydrometer method), the suspension of soil was dispersed with a dispersing agent to prevent flocculation and was permitted to settle in a cylinder (Fig. 4d). These hydrometer observations at definite intervals of time were employed to determine the concentration of particles remaining in suspension. The decreasing density of the suspension is measured at time intervals. Sizes were determined from the settling velocity and times recorded. Percentages between sizes were determined from density differences. About 30 to 50 g of the <0.063 mm sample that was collected in the buckets was put into a beaker with 25 cm^3 of the stock solution and thinned with 400 cm^3 purified water. The result was mixed up for about 20 minutes with the

mixer. After that, it was filled into the measuring cylinder and filled with purified water up to the 1000 cm³ mark. The suspension inside the measuring cylinder was homogenized by completely overturning the cylinder repeatedly for several minutes, but a run off was prevented. After shaking, the cylinder with its contents was placed on a desk, and at the same time, the stopwatch was started. The hydrometer was immersed carefully inside the suspension in a way that it swam without contacting the cylinder sides (Fig. 4d). After 30 seconds, 1, 2, 5, and 15 minutes, the reading above the meniscus was taken. After this time, the hydrometer was carefully taken out, rinsed with distilled water in the standing cylinder until the next reading. This was done to prevent soil particles from settling upon it, which can distort the readings. The next readings were purposefully taken after minutes and after 1, 2, 4, 6, and 24 hours. The suspension's temperature was measured once within the first 15 minutes, then directly after every reading according to the GGU-SIEVE program manual (Buß 2023).

Stokes' Law was applied to calculate the particle sizes from sediment speeds. Having the results from both methods, which were then used to construct a grain size distribution curve, resulted in a comprehensive particle size composition profile in the soils of the study area. It was the GGU-SIEVE program, which provides grain size curves and calculates soil classification parameters based on the German abbreviations for the soil type (Sand, silt, gravel, etc.). Significant soil properties such as D10, D20, D30, D50, and D60 diameters can be read from the curve for soil classifications. A grain size distribution curve is established by summing up the fractions (by weight), starting with the smallest fraction. A steep grain size distribution curve indicates a well-sorted sample; a flat curve indicates the opposite. After determining the D10, D30, and D60 from the semi-log grain size distribution curve, the GGU-SIEVE program determines the hydraulic conductivity of a soil sample using Hazen (1892), depending on the rules for how to use for soil texture, and clay content of the soil sample. After intensive sieving and sedimentation analysis in the laboratory, the estimation of the uniformity coefficient (Cu), coefficient of curvature (Cc), and the *K_Hazen* of the soils were carried out using the GGU-SIEVE program.

Grain size parameters determination using GGU-SIEVE

Each of the four methods in GGU-SIEVE relies directly or indirectly on grain size distribution parameters, particularly the uniformity coefficient (Cu) and coefficient of curvature (Cc), which the program automatically calculates from the inserted input data (for example, cumulative percent finer vs. grain diameter) that was obtained from the sieve analysis (Eqs. 1 and 2). These equations were also applied by Das (2013) and Davarpanah et al. (2025).

$$C_u = \frac{D_{60}}{D_{10}} \tag{1}$$

$$C_c = \frac{(D_{30})^2}{D_{10} \times D_{60}} \tag{2}$$

The D_{10} is the effective diameter (diameter at 10% finer), D_{60} and D_{30} are the grain diameters at which 60% and 30% soil samples are finer (by weight), respectively. Hazen primarily used D_{10} for estimating K, whereas he used Cu and

Cc only for checking the validity of the soil gradation. Soils with Cu < 5 and 1 ≤ Cc ≤ 3 were categorized as well-graded, whereas deviations from such ranges showed poorly graded, as highlighted by Cai et al. (2023).

Hydraulic conductivity determination using GGU-SIEVE

The hydraulic conductivity could be determined using hydraulic methods (Darcy's law) or correlation methods (pore size distribution, grain size distribution, soil texture, and soil mapping unit). As Cirpka (2003) pointed out, the characterization of the pore size diameters will be more appropriate than being concerned about the size of the grains. The determination of pore-size distribution is a complex task; therefore, hydraulic properties are usually approximated using grain size distribution, which is comparatively easier to measure. Hence, researchers have been trying to develop a relationship between permeability and particle size for many decades. Several formulae have been proposed over time to describe this relationship. The direct permeability testing or pedotransfer functions may be required to obtain more accurate hydraulic conductivity values for the fine-rich soils of lateritic materials. According to Vukovic and Soro (1992), the use of different empirical formulas on the same soil type gives permeability values that may differ by a factor of 10 or even 20 (Justine 2008).

Hydraulic conductivity values derived in this study were obtained from the GGU-SIEVE program using its optional hydraulic conductivity estimation tool. GGU-SIEVE offers multiple empirical formulas for estimating hydraulic conductivity from particle size distributions; however, unless otherwise specified, the software applies the Hazen (1892) relation using the D10 (10% of fines) grain-size as input. Because this estimation was requested during the initial data processing, our soils are predominantly sandy to silty sand with variable fine gravel content; the resulting hydraulic conductivity values correspond to the Hazen formulation (i.e., *K_Hazen*). It is vital to note that Hazen's method is only valid for clean, uniformly graded sands with minimal fines (0.1 to 3 mm). Seven of the lateritic soil samples analyzed in this study contain substantial fine fractions and do not strictly meet the applicability criteria. For this reason, all hydraulic conductivity values are treated as index values (*K_Hazen*) rather than absolute measurements, and are interpreted qualitatively.

After inserting required inputs and activating the "K values determination check-pox… the "Hazen method" setting is helpful, as the program then searches for this appropriate method. All required methods applied to determine grain size distribution, including sedimentation, sieve (wet and dry) analysis, grain size parameters (Cu, Cc), and estimation of hydraulic conductivities, are based on the GGU-software user's manual reported by Buß (2023).

Therefore, the GGU-SIEVE program effectively uses the Hazen's empirical equation (Eq. 1) to estimate hydraulic conductivity depending on the requirements, soil characteristics, and rules described by the GGU-Software developer.

Hazen method (1892):

$$K_Hazen = C_H \times D_{10}^2 \tag{3}$$

Where K is hydraulic conductivity (coefficient of permeability) (m/s), D_{10} is the effective grain diameter (10% finer size on grain size curve [mm or cm, depend-

ing on units]), and C_H is the empirical coefficient (usually between 100 and 150 when D_{10} in cm; or around 6×10^{-4} when D_{10} is in mm and it can be calculated as given in equation 4, where T also stands for temperature T (°C). This method is best suited for clean sand and uniform sand with a typical diameter ranging from 0.1 ≤, d10 ≤ 3 mm, as well as for Cu < 5.

$$C_B = \frac{0.07 + 0.03\mathrm{T}}{86.4} \tag{4}$$

Many scholars (Amadi et al. 2023; He et al. 2023; Panasa-Condensa 2024) categorized the soil permeability based on the order of magnitude of K (m/s) as very high (> 1×10^{-4}), high ($1 \times 10^{-5} - 1 \times 10^{-4}$), moderate ($1 \times 10^{-6} - 1 \times 10^{-5}$), low ($1 \times 10^{-7} - 1 \times 10^{-6}$), and very low (< 1×10^{-7}). The erosion potential (higher in highly permeable and poorly graded soils) was assumed based on the compositions of poor gradation and high hydraulic conductivity, which increases susceptibility to internal erosion and suffusion (Li 2014; Deng et al. 2023; Liu et al. 2025).

A variety of methods can be applied to describe and illustrate results obtained from grain size analysis. The most common way to present the distribution of grain sizes within a sample is to design a summation curve, where the arithmetic partition is plotted versus the grain size (Fig. 5). This kind of diagram is a simple and quick method to present a general characterization of the analyzed soils; because different parameters, e.g. sorting, can easily be obtained by the shape of the curve. A steep summation curve indicates a well-sorted sample, whereas a flat curve indicates a poorly sorted one.

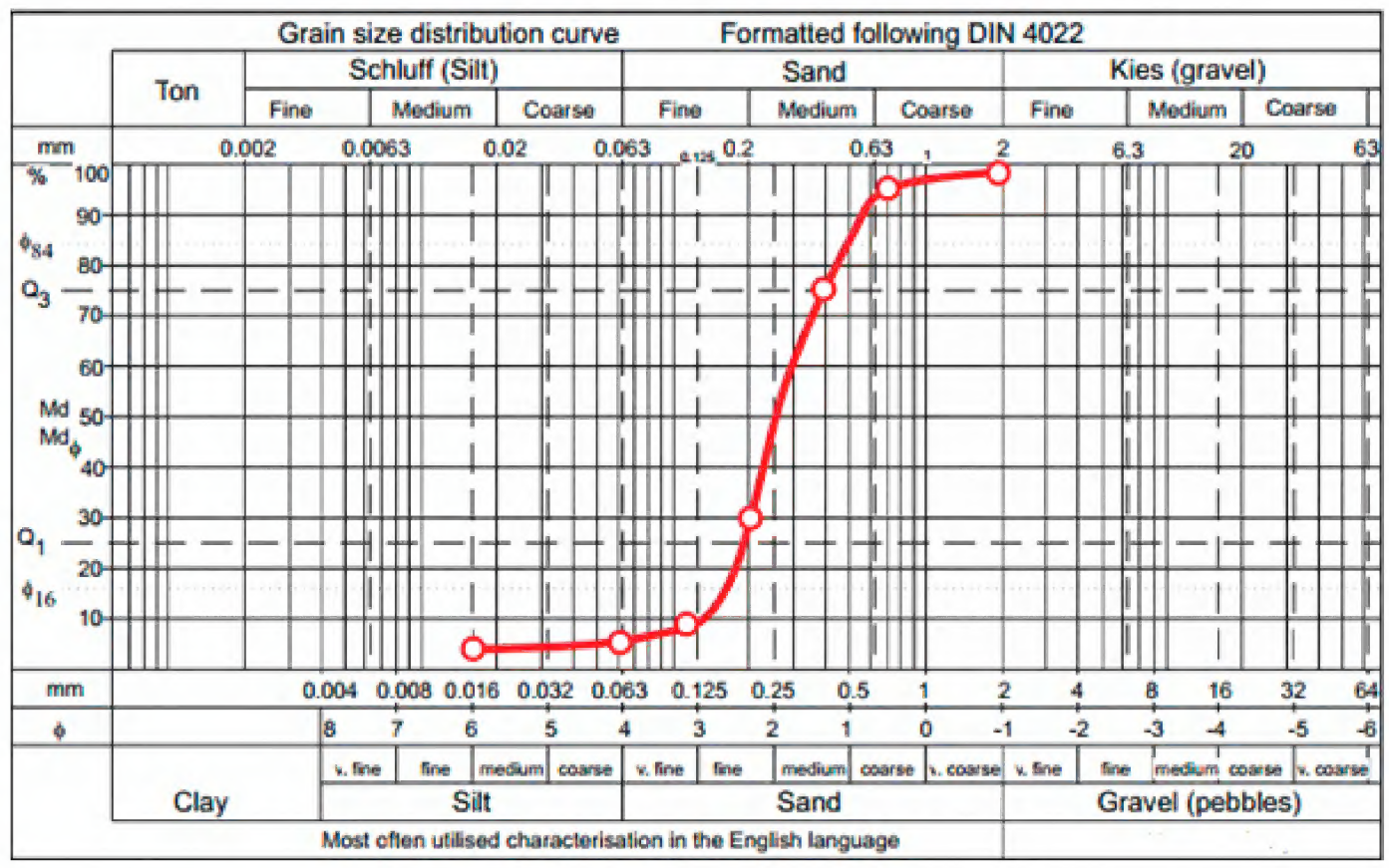

Figure 5. Sieve analysis for grain size distribution curve following the DIN 4022.

Statistical and comparative analysis

The analysis was carried out in Python using Pandas for data handling and Statsmodels for Ordinary Least Squares Model (OLS) and mixed-effects model. Matplotlib is also used for generating plots. The pairwise correlation analysis was used to analyze the heterogeneity across lithologies. In addition to the pairwise

analysis, further graphical and model analyses, including particle-size distribution curves grouped by lithology and residual and QQ plots, were implemented. We also performed ANOVA/Kruskal–Wallis tests for lithologic differences.

Results and discussion

In all, 24 soil samples from five weathered profiles, S1– S2, developed over different basement rocks of gneiss, gneiss-volcanics, quartzite, granite, and gneiss, were analyzed for the computation of soil parameters, such as Cu, Cc, and *K_Hazen*, with supplementary classification for permeability, gradation, and soil types, using the GGU-SIEVE program (Table 1). The textural classes of the analyzed soils are mainly dominated by sand to silty sand with varying fine gravel content (Table 1). The datasets were filled with 'na' (not applicable) to estimate the Cu, Cc, and K values by the GGU-SIEVE program due to the lack of the 10% fines. Hence, in our further analysis we use only 15 datasets for each of Cu, Cc, and K values.

Table 1. Summaries of soil characteristics, grain size parameters, and hydraulic conductivity (*K_Hazen*) for all 24 analyzed samples of five profiles.

Profile ID	Sample ID	Horizon depth (m)	Soil type (GGU-SIEVE-program)	Uniformity coefficient (Cu)	Coefficient of Curvature (Cc)	*K_Hazen* (m/s)
S1 (gneiss)	S1-1	0.9	S, fg	15	1.2	8.8×10^{-5}
	B1-2	2.1	S, u, t', fg'	na	na	na
	S1-3	3.1	U, t', fs', ms', gs', fg'	na	na	na
	S1-4	4.5	U, t', fs', ms', gs'	na	na	na
	S1-5	5.5	S, u, t'	36.2	1.1	2.0×10^{-7}
	S1-6	6.1	U, fs, ms, gs'	18.8	0.9	3.9×10^{-7}
S2 (gneiss-volcanics)	S2-1	0.6	fG, u, t', gs'	na	na	na
	S2-2	1.6	S, u, t', fg'	41.5	0.9	1.7×10^{-7}
	S2-3	3.3	S, u, fg	90.9	0.4	9.0×10^{-7}
	S2-4	4.8	S, u, fg	60	1.1	2.2×10^{-6}
S3 (quartzite)	S3-1	0.3	S, u, t', fg'	72.8	0.7	2.3×10^{-7}
	S3-2	2.5	S, u, t', fg'	na	na	na
	S3-3	5.4	S, t, u, fg	na	na	na
	S3-4	7	S, fg, u, t'	439	1.7	9.3×10^{-8}
S4 (granite)	S4-1	0.2	U, gs, fg, t', fs', ms'	65.5	0.2	2.1×10^{-7}
	S4-2	2.6	U, gs, fg, t', fs'	na	na	na
	S4-3	4.8	U, gs, fg, t', fs', ms'	na	na	na
	S4-4	7	S, fg, u, t'	344.3	1.8	2.4×10^{-7}
	S4-5	7.9	S, u, fg, t'	209.2	1.5	2.1×10^{-7}
S5 (gneiss)	S5-1	0.4	S, fg	17.5	1.8	1.3×10^{-4}
	S5-2	1.5	U, gs, fg, t', fs', ms'	228.3	0.3	5.8×10^{-8}
	S5-3	2.2	S, u, fg	84.7	0.9	7.2×10^{-7}
	S5-4	2.9	S, u, t', fg'	na	na	na
	S5-5	3.4	S, u, t', fg'	78.6	1.7	6.4×10^{-8}

Where GGU-SIEVE-program abbreviations are: na (not applicable), S (sand), U (Silt), t (clay), fg (fine sand), fs (fine sand or finer fraction), ms (medium sand), gs (coarse sand/gravel), u (non-uniform or heterogeneous grading), and primes (') after letters (e.g., t', fs') usually signify a minor presence.

The uniformity coefficient (Cu) among the profiles ranged widely, from 15 to 439, and evidenced large textural variability. The lowest Cu values, 15, occurred at the top layer of profile S1 and the highest, 439, in the deeper quartzite-derived profile S3. The mean Cu values for S1, S2, S3, S4, and S5 were approximately 23.3 ± 10.8, 64.1 ± 25.6, 255.9 ± 183.1, 206.3 ± 115.4, and 85.8 ± 84.2, respectively. The coefficient of curvature (Cc) varies between 0.2 and 1.8, but most are close to unity, representing a moderately well-graded material. The lowest value of Cc was 0.2 for the upper granite-derived sample S4-1, while the highest was 1.8 for both S4 (in S4-4) and S5 (in S5-1) profile samples (Table 1).

The values of *K_Hazen* ranged from 9.3×10^{-8} m/s to 1.30×10^{-4} m/s covering nearly four orders of magnitude. The maximum value (1.30×10^{-4} m/s) was found in the upper gneiss soil (S5-1), and the minimum (9.30×10^{-8} m/s) was in the quartzite profile (S3-4) (Table 1). The order of mean *K_Hazen* among the profiles was S5 (4.5×10^{-6} m/s) > S1 (3.6×10^{-6} m/s) > S2 (1.1×10^{-6} m/s) > S4 (2.2×10^{-7} m/s) > S3 (1.6×10^{-7} m/s). Standard deviations were highest in profile S5, demonstrating larger intra-profile variability. Soil hydraulic conductivity (*K_Hazen*) is one of the major parameters controlling the movement of water in soil and affects the formation of surface runoff. Soils with low *K_Hazen* are prone to saturated-excess runoff, which causes overland flow and increased potential for sheet, rill, and gulley erosion. The variations of observed *K_Hazen* values within the soil profiles suggest variation in infiltration rates, which are closely linked to soil texture and grading. These findings are consistent with the explanation provided by Ali et al. (2012), who argue that hydraulic property and grain size parameter distributions affect the sediment transport capacity in overland flow.

Cu and Cc values led to the soils being classified as moderately to well-graded sands, except for some gap-graded distributions for the granite (S4-1) and gneiss-volcanics (S2–3) layers. The corresponding permeability classes, developed from *K_Hazen* values, ranged from low (10^{-8} m/s) to high (10^{-4} m/s). Profiles S1 and S5 showed moderate to high permeability in their surface horizons. The S3 and S4 soil profiles were dominated by low-permeability horizons across their depth. The S2 soil profile indicated a moderate permeability that progressively increased with depth.

Correlation analysis

The statistical appraisal of subsurface grain-size characteristics and hydraulic conductivity shows several noteworthy trends that link directly to the geological context of the different basement lithologies. The pairwise correlations indicate moderate positive associations between Cu and depth ($r = 0.55$, $p < 0.05$), and between Cc and depth ($r = 0.48$, $p = 0.07$), while $\log_{10}(k)$ indicates a weak and statistically insignificant relationship with these grain-size metrics ($r = 0.22$ for Cc, $r = -0.45$ for Cu). These relations are visualized in the correlation matrix (Table 2), which summarizes the reliance structures among variable and highlights the modest predictive connection between hydraulic conductivity and grain-size characteristics.

Table 2. Summary of pairwise correlation analysis (r, p, n = 15) results for soil parameters.

Variable 1	Variable 2	Cor. Coefficient (r)	Significant level (p)	Interpretation
Depth (m)	Cu	**0.55**	**0.03**	Moderate positive, statistically significant
Depth (m)	Cc	0.48	0.06	Moderate positive, marginal significant
Depth (m)	log10_k	-0.36	0.18	Weak negative, not significant
Cu	Cc	0.33	0.22	Weak positive, not significant
Cu	log10_k	-0.45075	0.09	Moderate negative, borderline significant
Cc	log10_k	0.22	0.42	Weak positive, not significant

Model evaluation and comparison for hydrogeological interpretation

The simple bivariate patterns underlying these correlations are further illustrated in the exploratory scatter plots of $\log_{10}(k)$ versus depth (Fig. 6a) and $\log_{10}(k)$ versus Cu (Fig. 6b), which shows considerable scatter and heterogeneity across lithologies. These visualize patterns indicate that while some trends exist, subsurface variability is too complex to be captured using simple linear

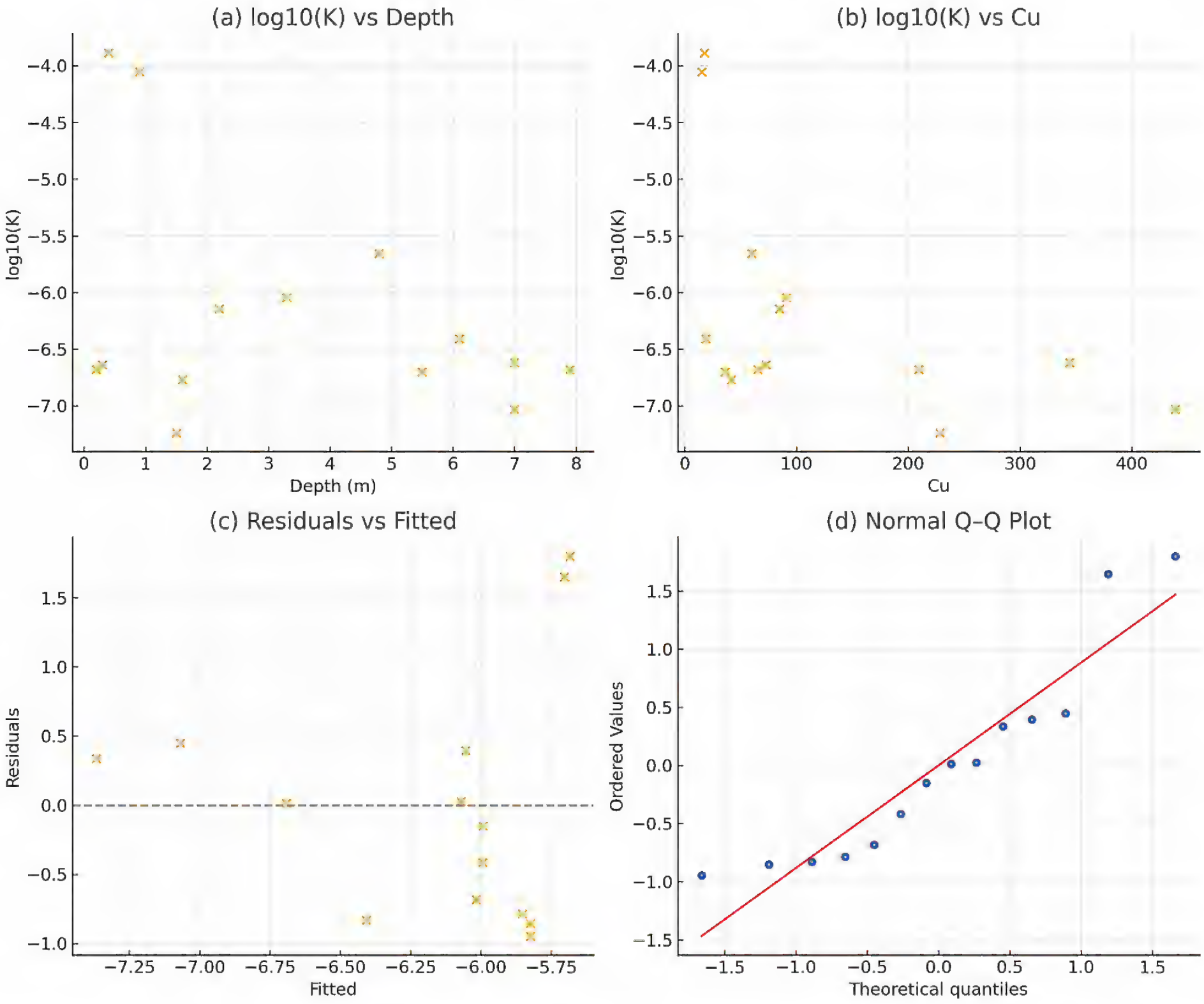

Figure 6. Plots illustrating statistical and model-based relationships among soil properties: **a.** $\log_{10}(k)$ vs. depth; **b.** $\log_{10}(k)$ vs. Cu and models: **c.** Residual vs. fitted; and **d.** Normal Q-Q plot.

relationships alone. Note that for the next considerations of $\log_{10}(k)$ and K, these represent K values that are the values of *K_Hazen* through modeling and comparisons of the soil samples.

Model performance was then assessed for a set of linear and mixed-effects models that progressively incorporated Cu, Cc, and lithology, with profile ID treated as a random effect where appropriate. Comparisons based on Akaike Information Criterion (AIC), Bayesian information criterion (BIC), and Log-Likelihood (LLF) (Table 3) indicate that models with fewer parameters are generally performing better, suggesting limited explanatory gain from additional covariates or hierarchical structure given the dataset available.

Table 3. Model comparison and selection statistics for alternative regression and mixed-effects models using BIC, AIC, and LLF, and number of model parameters (n). Lower AIC and BIC varies indicate better model fit.

Model Name	Description	Akaike information criterion (AIC)	Bayesian information criterion (BIC)	Log-Likelihood (LLF)	No of estimated parameters
Ordinary Least Squares Model (OLS)	Base linear regression model	47.92	50.76	-19.96	4
Ordinary Least Squares Model with additional predictors (OLS-2)	Extended linear model including an extra variable	48.45	51.99	-19.23	5
Mixed-effects model 0 (M0)	Random-intercept model	48.04	50.17	-21.02	2
Mixed-effects model 1 (M1)	Random intercept + lithology as fixed effect	52.56	56.80	-20.28	5
Mixed-effects model 2 (M2)	Random-intercept + lithology and depth interactionl	52.78	57.73	-19.39	6

Diagnostic consideration was critical in explaining these differences. These Residuals versus Fitted plot (Fig. 6c) indicates that the more parameterized models (m1 and m2) display structured residual patterns and mild heteroscedasticity, while the simpler formulations (m0 and OLS) show more consistent residual scatter, which supports their higher rankings on the basis of AIC/BIC. The Normal Q-Q Plot (Fig. 6d) further illustrates that residuals from the simpler models adhere more closely to the theoretical quantile line, indicating that their error distributions better meet the assumptions of linear modeling. Additional diagnostic views, including scale-location and leverage plots (Fig. 7a), similarly confirm that the simple models lack influential outliers and maintain more consistent variance patterns.

These statistical trends take on clearer geological significance in light of lithologic differences among the various profiles. K varies both within and among the lithologies; gneiss-derived profiles are more heterogeneous in grain-size, consistent with mixed metamorphic weathering, whereas quartzite and granite generally yield more uniform sands. These distinctions are preserved in the grouped relationship plot of $\log_{10}(k)$ vs. depth by lithology (Fig. 7b), wherein conductivity decreases with depth in several lithologies-most dramatically in gneiss. Hydrogeologically, such a trend could result from compaction, increased fines content, deeper weathering profiles, or structurally induced permeability reductions. The poor statistical correlation between the gran-size coefficients (Cu, Cc) and *K_Hazen* likely result from this complexity of lithology and structural rather than from random measurement variability.

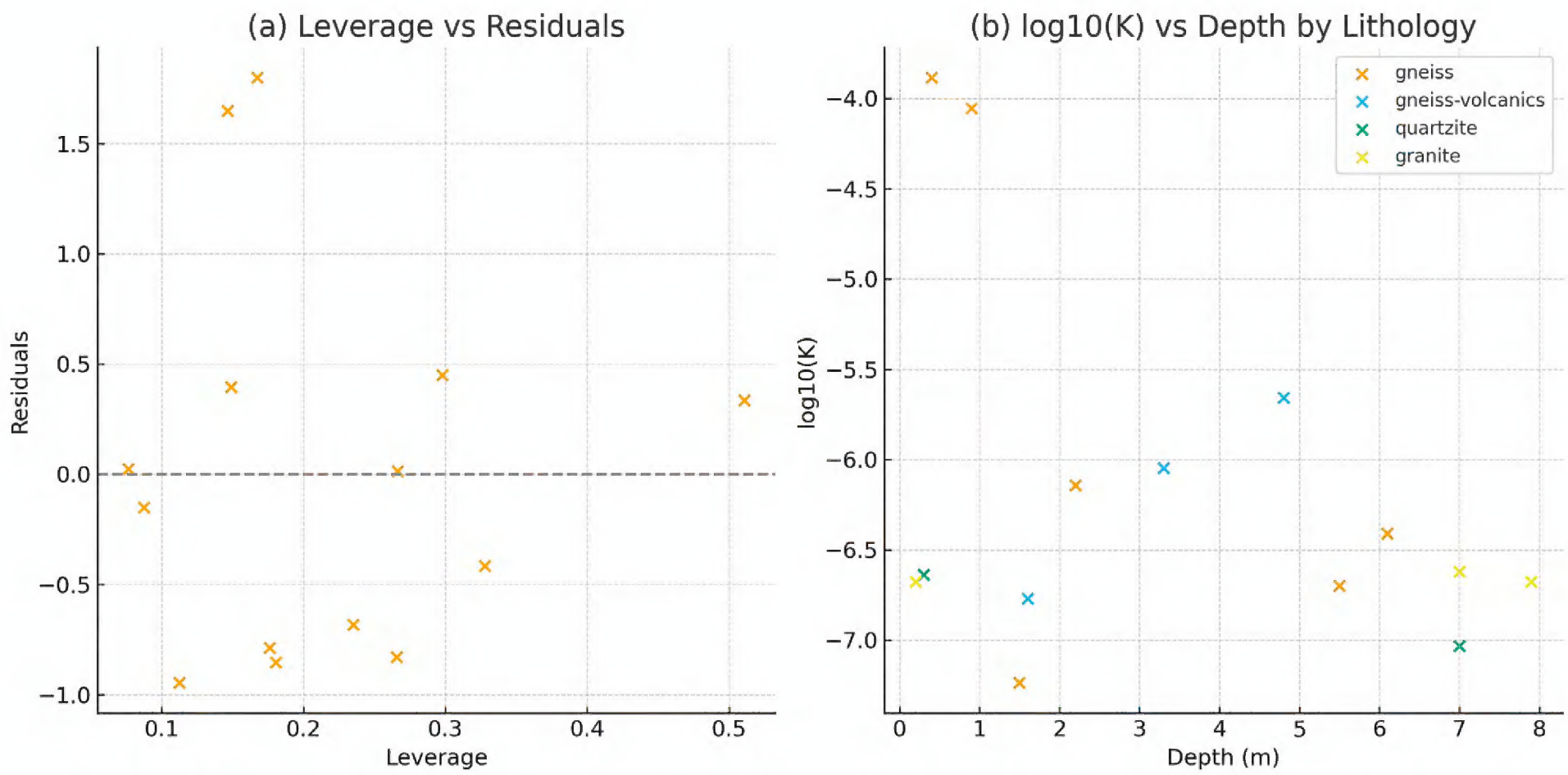

Figure 7. Illustrating: **a.** The influence plot (Leverage vs. Residuals) and **b.** Grouped relationships $\log_{10}(k)$ vs. depth by lithology.

In summary, these exploratory plots, diagnostic evaluations, and model comparisons suggest that: 1) lithology and depth are meaningful controls on hydraulic conductivity (*K_Hazen*); 2) simpler regression structures outperform the more complex mixed-effects models due to limited within-profile replication; and geological heterogeneity in this setting dominates subsurface hydraulic behavior. While Cu represents the grain-size parameter most consistently related to *K_Hazen*, increased sampling-especially deeper and with increased profile-level replication-would better allow mixed-effects models to consider the full geologiac hierarchy and to partition variations more appropriately across lithologic units.

Beyond the statistical and hydrogeological interpretations, such findings also have implications for the management of downstream estuaries. Given that lithology determines soil texture, grain-size distribution or grading indices, and hydraulic conductivity, it controls the relative balance between surface runoff and subsurface flow across the catchment. Coarser quartzitic soils could allow more infiltration, lowering sediment export, whereas finer gneissic and grantic soils are more capable of generating runoff and transporting sediment during storm events. Such contrasts form fundamental or first-order controls on the quantity and timing of sediment and solute fluxes delivered to downstream waterways and ultimately, to estuaries. While this study does not seek to quantify explicitly hillslope-to-estuary fluxes, the general lithology-soil-property relationships identified herein provide essential upstream constraints that may be factored into catchment-scale management planning in future sediment-transport or estuarine-vulnerability assessments.

Conclusions

This study distinguishes the underlying effect of basement rock on soil physical and hydraulic properties of lateritic soils using the GGU-SIEVE program analysis, which demonstrates that soil textural and hydraulic properties in

basement-derived profiles differ systematically with lithologic and depth. These gneissic-derived soils, S1 and S5, are moderately to well-graded (Cu ranges from 15 to 228), showing the highest surface hydraulic conductivity (*K_Hazen*) (up to 10^{-4} m/s), reducing abruptly with depth. The soils derived from gneiss-volcanics (S2) showed heterogeneous grading uniformity coefficient (Cu) up to 91 and moderate *K_Hazen* between 10^{-7}–10^{-6} m/s, reflecting their mixed mineralogical and weathering influences. Quartzite- and granite-derived soils, S3 and S4, show extreme gradation, with Cu > 200, but hydraulic conductivity (*K_Hazen*) is low in the range of 10^{-8}–10^{-7} m/s, because of dense packing or compaction and fine infilling. The statistical analysis and modeling diagnostics datasets reveal that parent rock composition and the degree of weathering have a dominant control on soil gradation, structure, and *K_Hazen*. Hydraulic conductivity (*K_Hazen*) generally declines with increasing depth, fines, and compaction, whereas erosion vulnerability rises with coarser horizon textures. Integration of Cu, Cc, and K results offers a reliable framework for evaluating soil permeability and erosion intensity in weathered basement terrains. These findings are useful in soil conservation planning, slope stability analysis, foundation design, and groundwater recharge modeling within the basement complex region. Consequently, future research will be directed at coupling these sieve- and hydrometric-derived soil parameters with in situ infiltration tests, grain-size distribution analysis, and mineralogical characterization to refine empirical correlations between uniformity coefficient, coefficient of curvature, and coefficient of permeability. An advanced geostatistical mapping or numerical flow model of K across lithological limits could improve the geospatial prediction of subsurface hydrological behavior. The long-term monitoring of soil hydraulic changes under varying land use and climatic conditions would also help evaluate erosion response and permeability evolution in weathered basement environments.

Acknowledgements

The author wishes to express his thanks to Mekelle University and TU Darmstadt for providing a free soil laboratory during my MSc and scientific training work, respectively. And similar thanks for the laboratory workers as well as to the university authority for their support during my work.

Additional information

Conflict of interest

The author has declared that no competing interests exist.

Ethical statement

No ethical statement was reported.

Use of AI

No use of AI was reported.

Funding

No funding was reported.

Author contributions

The author solely contributed to this work.

Data availability

All of the data that support the findings of this study are available in the main text.

References

Ali M, Sterk G, Seeger M, Boersema M, Peters P (2012) Effect of hydraulic parameters on sediment transport capacity in overland flow over erodible beds. Hydrology and Earth System Sciences 16: 591–601. https://doi.org/10.5194/hess-16-591-2012

Amadi AA, Osinubi KJ, Okoro JI (2023) Hydraulic conductivity of unsaturated specimens of lateritic soil bentonite mixtures. Geotechnical Engineering 41: 4431–4444. https://doi.org/10.1007/s10706-023-02524-3

Biru MK, Gadisa CW, Dirbaba NB, Nunes MR (2025) Land use changes and their impacts on soil erosion in fragile ecosystem of the Ethiopian highlands. Land 14(7): 1473. https://doi.org/10.3390/land14071473

Brown D, Clayton MK, McSweeney K (2004) Potential terrain controls on soil color, texture contrast and grain-size deposition for the original catena landscape in Uganda. Geoderma 122(1): 51–72. https://doi.org/10.1016/j.geoderma.2003.12.004

Buß J (2023) Evalation and presentation of Sieve and hydrometer analysis to DIN 1123 and DIN EN ISO 1792-4, GGU-SIEVE Version 17: 1–64. https://www.ggu-software.com/fileadmin/products/manuals/GGU-SIEVE_man-e.pdf

Cai Z, Chen Y, Zhu X, Tang Y (2023) Influence of gradation on particle breakage and deformation characteristics of coral sand. Chinese Journal of Geotechnical Engineering 45(4): 661–670. https://doi.org/10.11779/CJGE20220884

Cirpka OA (2003) Environment Fluid Mechanics I: Flow in Natural Hydrosystems.

Colin F, Brimhall G, Nahhon G, Lewis CJ, Baronnet A, Danti K (1992) Equatorial rainforest lateritic soils, A geomembrane filter. Geology 20: 523–526. https://doi.org/10.1130/0091-7613(1992)020%3C0523:ERFLMA%3E2.3.CO;2

Das BM (2013) Principles of Geotechnical Engineering. Cengage Learning.

Davarpanah SM, Narimani S, Sharghi M, Vásárhelyi B (2025) Introducing coefficients of curvature (Cc) and uniformity (Cu) based on RQD for rock mass characterization. Rock Mechanics Letters 2(1): 10. https://doi.org/10.70425/rml.202501.10

Deng Z, Chen X, Jin W, Wang G (2023) Effect of gradation characteristics and particle morphology on internal erosion of sandy gravels. Water 15(14): 2066. https://doi.org/10.3390/w15142660

Etim EE, Ibe KM, Ufot UO (2025) Grain size distribution and hydraulic conductivity evaluation of tropical soils from basement rocks. Journal of African Earth Science 211: 104895.

Fajobi MA, Aladejana JA, Oyedele DJ (2014) Hydraulic properties and erodibility of selected Nigerian soils. African Journal of Agricultural Research 9(12): 991–998.

Fukushima Y, Masaki T, Nakamura R (2021) Hydrological impacts of soil physical properties in coastal and estuarine catchments. Journal of Hydrology 600: 126672.

Hazen A (1892) Some Physical Properties of Sands and Gravels, with Special Reference to their Use in Filtration. 24th Annual Report of the Massachusetts State Board of Health, Pub. Doc. No. 34: 539–556.

He K, Zhang Q, Ai Z, Xu N, Qiao Y, Tian C, Leng P, Cheng H, Chen G, Li F (2023) Characteristics and influence factors of soil water and salt movement in the yellow river irrigation district. Agronomy 14(1): 92. https://doi.org/10.3390/agronomy14010092

Justine O (2008) Evaluation of empirical formulae for determination of hydraulic conductivity based on grain-size analysis. The Journal of American Science 4(1): 1–6.

Lee J, Smith A, Wong D (2024) Weathering profile of completely weathered rock from the Dullstroom Formation, south Africa. Bulletin of Engineering Geology and the Environment 83: 1–12. https://doi.org/10.1007/s10064-025-04224-z

Li WB (2014) Study on the permeability characteristics of coarse-grained soil and its permeability rule. Advanced Materials Research 904: 383–388. https://doi.org/10.4028/www.scientific.net/AMR.904.383

Li Y, Wang C, Zhang X (2019) Influence of soil properties on groundwater recharge and pollutant transport in estuarine environments. Environmental Monitoring and Assessment 191(5): 279.

Liu C, Zhang Z, Cheng L, Wang Y, Liu X, Lai R, Lyv Q (2025) Effects of soil particle size on rainfall-induced erosion of near-horizontal layered slopes. PLOS ONE 20(9): e0331153. https://doi.org/10.1371/journal.pone.0331153

Muller D, Bocquier G, Nahon D, Pacquet H (1981) Analyse des differentiations mineralogiques et structurales d'un sol ferralitique a' horizons nodulaires du Congo. Cahiers O.R.S.T.O.M.: Série pédologie 18: 87–109.

Nyende J, van Tonder G, Vermeulen D (2014) Geological evolution of low lying areas in Uganda: Impacts of climate variability on rock weathering and consequences on groundwater quality and availability-review. Journal of Environmental Science and Water Resources 3(8): 163–183.

Obiefuna JN, Nur A (2022) Soil erosion and land degradation in the humid tropics: A review of key physical factors. Environmental Research and Public Health 19(4): 2134.

Omara P, Muvunyi M, Nanyunja D (2018) Basement geology and soil development in Western Uganda: implications for water resource management. Journal of African Earth Science 145: 123–130. https://doi.org/10.1016/j.jafrearsci.2018.06.011

Panasa-Condensa (2024) Revised soil classification system for coarse-fine mixtures. https://ponasa.condesan-ecoandes.org

Schlüter T (2006) The Geological Atlas of Africa; with Notes on Stratigraphy, Tectonics, Economic Geology, Geohards, Geosites and Geoscientific Education of Each Country (2nd Edition).

Tang Y, Lin H, Zhou M (2022) Role of soil texture in estuarine sediment deposition and water quality management. Estuarine, Coastal and Shelf Science 265: 107689.

Taylar RG, Howard KWF (1999) Lithological evidence for the evolution of weathered mantles for the evolution in uganda by tectonically controlled cycles of deep weathering and stripping. Antorio: Groundwater Research Group, Department of Geology, Uniĺersity of Toronto, 1265 Military Trail. https://doi.org/10.1016/S0341-8162(98)00118-0

Vukovic M, Soro A (1992) Determination of Hydraulic Conductivity of porous media from grain-size compaction. Water Resources Publications, Littleton, Colorado.

Waleed M, Inam MA, Albano R, Samad A, Farid HU, Shoaib M, Ali MU (2025) Statistical model development for estimating soil hydraulic conductivity through on-site investigations. Hydrology 12(3): 55. https://doi.org/10.3390/hydrology12030055